MASTER THESIS

Prediction of the nonlinear dynamic behaviour of a concrete slab subjected to blast load

Appendix II – Validation experiment 2

Author: L. Kraaijenbrink

Status: Final

Date: 11 July 2022

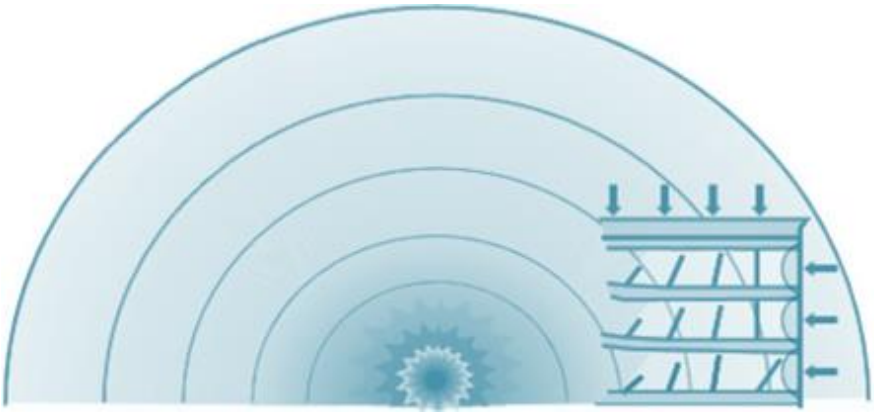

TU Delft

Royal HaskoningDHV
Enhancing Society Together

Open

HASKONINGDHV NEDERLAND B.V.

George Hintzenweg 85
3068 AX Rotterdam
Industry & Buildings
Trade register number: 56515154

+31 88 348 90 00 **T**
info@rhdhv.com **E**
royalhaskoningdhv.com **W**

Document title:	Prediction of the nonlinear dynamic behaviour of a concrete slab subjected to blast load	
Subtitle:	Appendix II – Validation experiment 2	
Status:	1.0/Final	
Date:	11 July 2022	
Author(s):	ing. L. Kraaijenbrink	
Thesis committee:	Prof.dr.ir. J.G. Rots	TU Delft
	Prof.dr.ir. M.A.N. Hendriks	TU Delft
	Dr.ir. K.N. van Dalen	TU Delft
	P.J. Flink	Royal HaskoningDHV

Table of Contents

1 Introduction

This appendix presents the results of the experiment conducted in Woomera, Australia in 2004 (Ngo, Mendis, & Krauthammer, 2007). The goal of the experiment is to investigate the structural behaviour of concrete for heavy explosions. The explosion is captured and shown in Figure 1.1. The crater that is left behind is massive, showing the impact of such explosions.

The blast was generated by a 6 t TNT equivalent explosion with a standoff distance of 40 m. This is equivalent to the scaled distance Z of 2.3 m/kg$^{1/3}$, high enough to be considered ‘far field’.

Figure 1.1: Installing panels into concrete frames (top left), Panels ready for blast (top right), Blast, equivalent to 6t of TNT (bottom left), Crater (17m diameter) caused by the blast (bottom right)

The panel of interest is shown in Figure 1.2. Conventional concrete and reinforcement are used in the panel.

Figure 1.2: Panel 4 before the blast

2 Experiment results

The obtained results in the experiment are presented in this chapter. The goal is to recreate these results in the FDM model.

2.1 Observations

There is no displacement-time history graph available for panel 4. Some observations are described in (Ngo, Mendis, & Krauthammer, 2007):

- Concrete is spalled off on the front face, which leaves a cavity of 100 mm width and 30 mm depth.
- A permanent deflection of 142 mm is measured.
- At the rear surface, an approximately 8-mm-wide crack at the midspan is observed.

The concrete panel after the blast trial is shown in Figure 2.1. Figure 2.2 is a scaled illustration of the observations. At the given permanent deflection, the support rotation is 8°.

Figure 2.1: Panel 4 after the blast

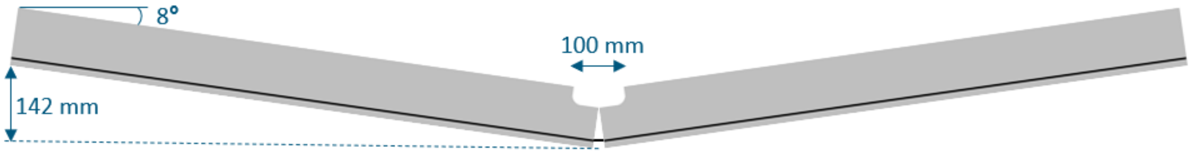

Figure 2.2: Scaled illustration of the observations

3 Parameters

The parameters in the dynamic analysis are strain rate dependant. The strain rate is extracted from the analysis. An average value for the strain rate is used according to (3.1) and (3.2), where t_E is the time to yield the reinforcement bars.

$$\dot{\varepsilon}_{c,avg} = 0.002/t_E \tag{3.1}$$

$$\dot{\varepsilon}_{s,avg} = f_{dy}/(E_s t_E) \tag{3.2}$$

Table 3.1: Dynamic parameters

Parameter	Units	Panel 4
Time to yield t_E	s	0.0065
Concrete strain rate $\dot{\varepsilon}_{c,avg}$	s^{-1}	0.308
Steel strain rate $\dot{\varepsilon}_{s,avg}$	s^{-1}	0.5
DIF_c	-	1.25
DIF_t	-	1.46
DIF_E	-	1.27
DIG_{GF}	-	1.00
DIF_{GC}	-	1.25

The concrete properties, which are based on an element length of 41.67 mm, are included in Table 3.2. The steel reinforcement properties are provided in Table 3.3.

Table 3.2: Concrete properties

Parameter	Units	Panel 4
Young’s modulus (static / dynamic)	MPa	33296 / 42285
Initial Poisson’s ratio	-	0
Mass density	Kg/m^3	2400
Tensile curve	-	Hordijk
Tensile strength (static/dynamic)	MPa	3.01 / 4.40
Fracture energy	N/m	137
Poisson’s ratio reduction	-	Damage based
Compression curve	-	Parabolic
Compressive strength	MPa	39.80 / 49.75
Compressive fracture energy	N/m	35419 / 44274

Table 3.3: Steel reinforcement properties

Parameter	Units	Panel 4
Young’s modulus	MPa	200000
Yield stress (static / dynamic)	MPa	550 / 645
Ultimate engineering stress (static / dynamic)	MPa	594 / 691
Ultimate engineering strain	-	0.05

The applied concrete and reinforcement stress-strain relationships are shown in Figure 3.1 and Figure 3.2, respectively.

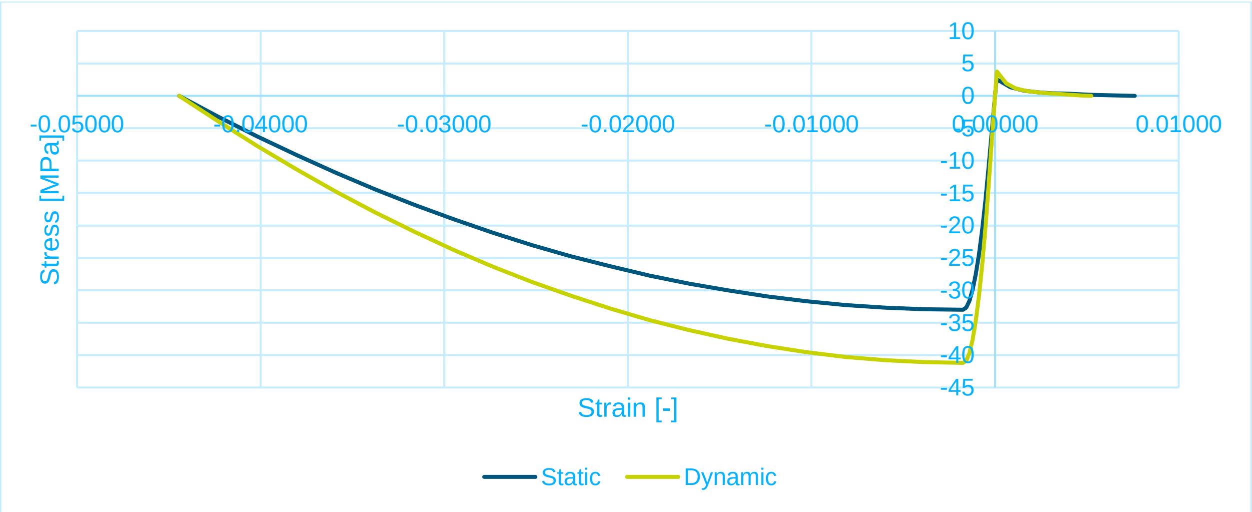

Figure 3.1: Concrete stress-strain relationship for the element length of 41.67 mm

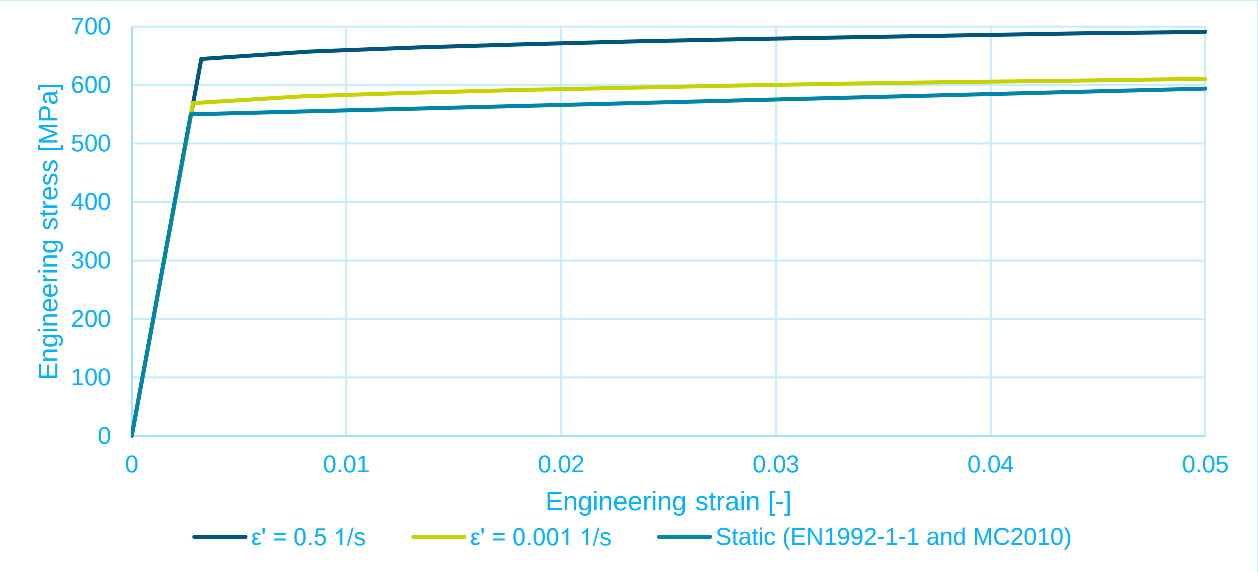

Figure 3.2: Reinforcement stress-strain relationship for panel 4

4 Applied force

The measured reflected pressure is shown in Figure 4.1. The simplification of the measured pressure is indicated in the figure and is approximated by (4.1). The approximating function is shifted by -32.5 ms in Figure 4.1.

$$DIF_t = \begin{cases} 700 - 700\dfrac{t}{5.25} & \text{for } 4.5\ ms \geq t \geq 0 \\ 116 - 116\dfrac{t}{32.5} & \text{for } 32.5\ ms \geq t \geq 4.5\ ms \end{cases} \tag{4.1}$$

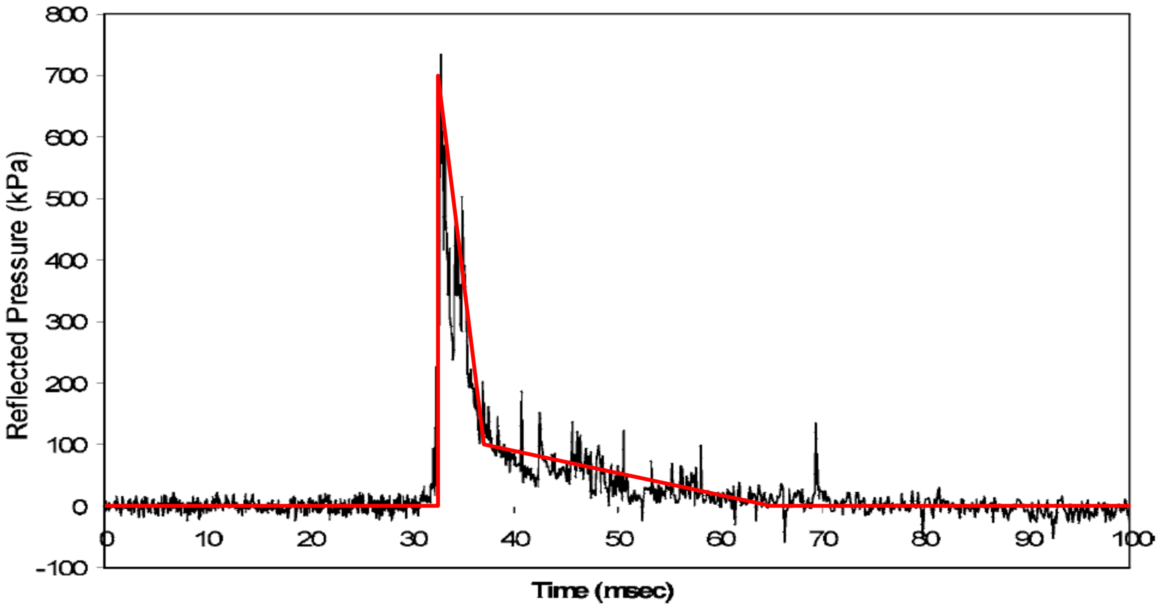

Figure 4.1: Applied pressure on Panel 4

5 Dynamic analysis with FEM comparison

In this chapter, the results of the FDM analyses are presented. A comparison is made with the FEM results.

5.1 Moment curvature relationship

The Moment-curvature (M-κ) graph is manually constructed and shown in Figure 5.1 and more specified in Table 5.1. Noticeable is that the manually constructed M-κ graph fails earlier than the M-κ graph obtained in FEM. This is because the concrete crushes before the reinforcement fails, whereas the failure mechanism in the FEM analysis is reinforcement failure. The stress state at the onset of failure (crushing) is shown in Figure 5.2. It is retrieved from the python script behind the manually constructed M-κ graph.

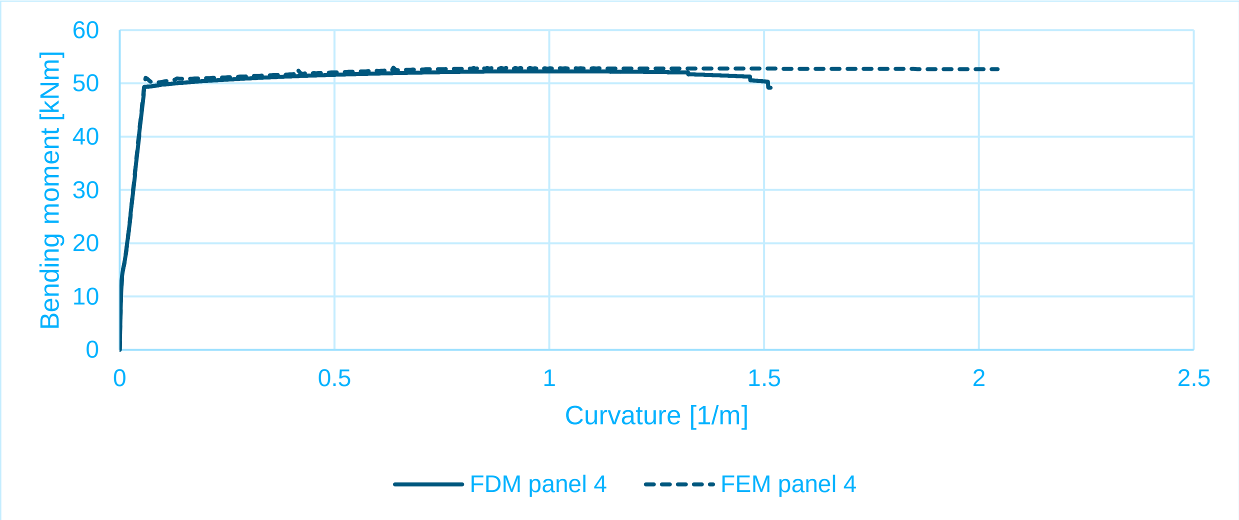

Figure 5.1: M-κ graph for panel 4

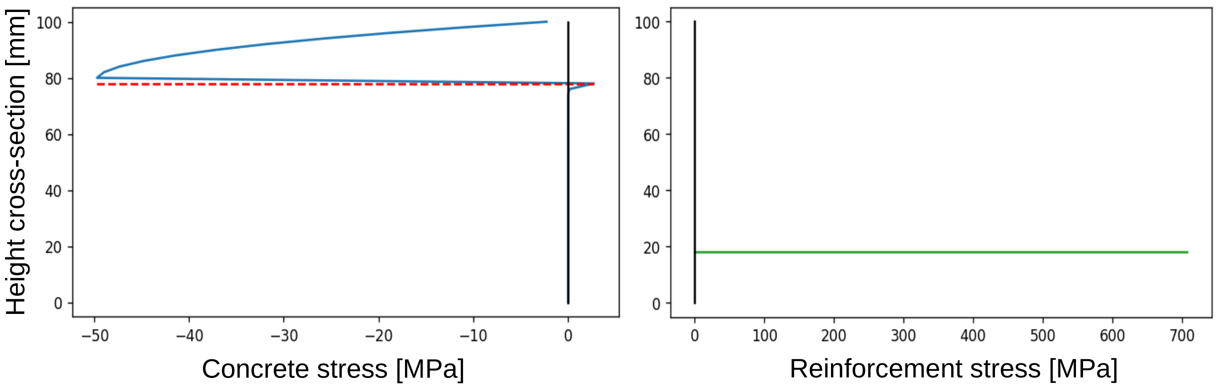

Figure 5.2:Stress state in the cross-section at the onset on failure

Table 5.1: Values for the distinct points in the M-κ graph

	Units	Panel 4
Cracking bending moment	kNm	7.76
Cracking curvature	1/m	0.00208
Yielding bending moment	kNm	49.36
Yielding curvature	1/m	0.0576
Ultimate bending moment	kNm	52.27
Ultimate curvature	1/m	1.52

5.2 Force-deflection relationship

The force-deflection (F-u) is shown in Figure 5.3 and more specified in Table 5.2: Values for the distinct point in the F-u graph. The permanent deflection is 142 mm, which does not lead to failure according to the F-u graph.

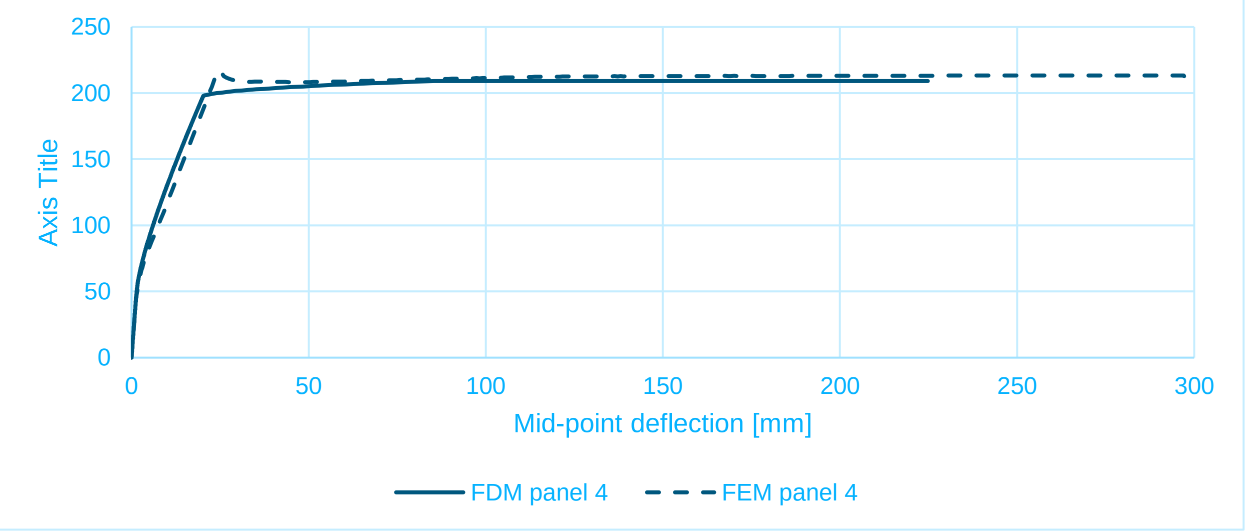

Figure 5.3: F-u graph for panel 4

Table 5.2: Values for the distinct point in the F-u graph

	Units	Panel 4
Cracking force	kN	31.36
Cracking deflection	mm	0.878
Yielding force	kN	197.81
Yielding deflection	mm	20.25
Ultimate force	kN	209.10
Ultimate deflection	mm	224.80

5.3 Single degree of freedom mass-spring system

The result of the mass-spring system analysis is shown in Figure 5.4.

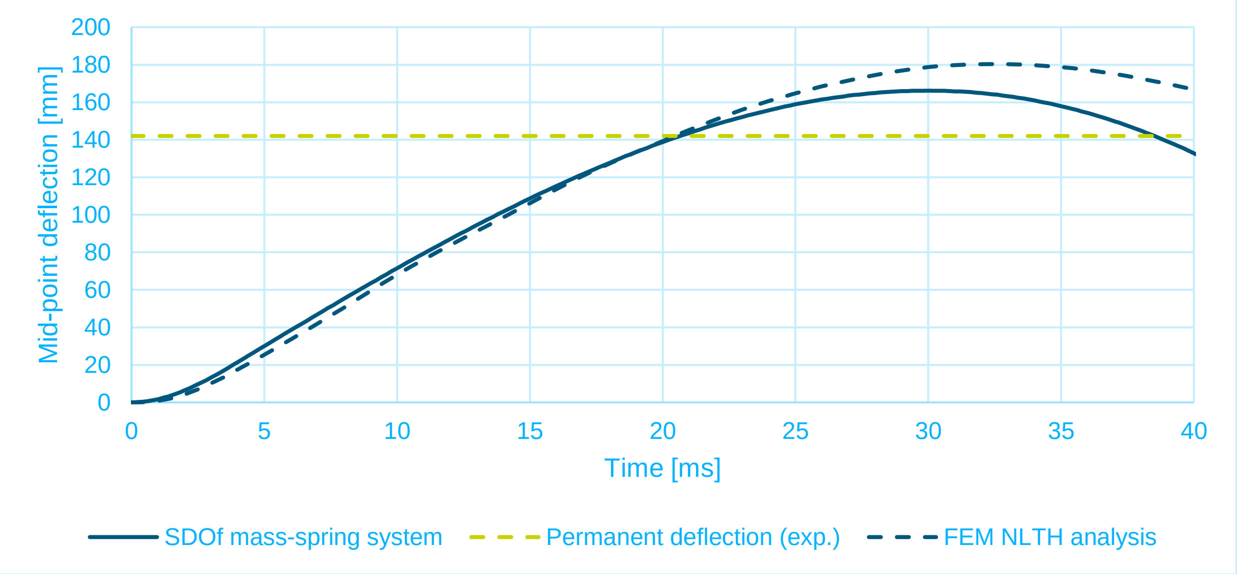

Figure 5.4: Deflection-time history graph of the mass-spring system

6 Discussion

The results of the SDOF mass-spring system are close to the results of the nonlinear time history analysis performed in DIANA. The deflection goes beyond the permanent deflection, which is as expected. Due to the inward acceleration after reaching the maximum deflection and possible effects of the negative phase of the blast (partial vacuum), the slab moves back.

UFC 3-340-02 emphasizes on multiple occasions that crushing may occur at the support rotation of 2 degrees. This experiment shows that this is a rather conservative assumption since the support rotation goes up to 8 degrees. A comprehensive study is performed by (U.S. Army Corps of Engineers, 2008) on the comparison of SDOF analysis to a large data set of experiments (Table 6.1). The referred test series in (U.S. Army Corps of Engineers, 2008) are mostly classified since they were conducted by defence departments. The study gives a good indication of the level of damage at certain support rotations. Up to 2 degrees the damage of the element could be considered moderately. Above the support rotation of 2.6 degrees the damage level is categorised as “heavy” damaged. The transition zone between 2 degrees and 2.6 degrees could lead to “moderate” damage or “heavy” damage. The crucial part of this study is that it shows the ductility of one-way elements beyond the support rotation of 2 degrees up to 6 degrees. This confirms the observations made on the ductility of one-way elements in the validation experiments.

Table 6.1: SDOF analysis on a large data set (U.S. Army Corps of Engineers, 2008)

Test Series	Test No.	L	Thick (inch)	Depth (inch)	f'dc (psi)	fdy (psi)	Reinf. Ratio (%)	Reinf. Index	Support	Weight (psi)	Ieff (in^4/in)	E (psi)	M (lb-in/in)	Ru (psi)	K (psi/in)	Mass (psi-ms^2/in)	P (psi)	I (psi-ms)	Pbar	Ibar	Max. Defl. (inch)	Theta (deg)	Damage Level
Scaled Testing, Analysis of Building Components	F1	250	7.9	6.7	8000	8.5e4	0.66	0.069	Simple	0.68	20.3	5.1e6	2.4e4	3.0	2.0	1753	42	212	13.8	0.09	5.2	2.4	Heavy
	F3	250	7.9	6.7	8000	8.5e4	0.66	0.069	Simple	0.68	20.3	5.1e6	2.4e4	3.0	2.0	1753	15	140	4.9	0.06	2.5	1.2	Moderate
	F4	250	7.9	6.7	8000	8.5e4	0.66	0.069	Simple	0.68	20.3	5.1e6	2.4e4	3.0	2.0	1753	7	72	2.3	0.03	0.8	0.4	Moderate
	F5	250	7.9	6.7	8000	8.5e4	0.66	0.069	Simple	0.68	20.3	5.1e6	2.4e4	3.0	2.0	1753	166	350	54.4	0.16	7.9	3.6	Heavy
	F6	250	7.9	6.7	8000	8.5e4	0.66	0.069	Simple	0.68	20.3	5.1e6	2.4e4	3.0	2.0	1753	4	32	1.1	0.01	0.3	0.1	Superfcl
	P1-shot 1	250	5.3	4.5	8000	8.5e4	0.66	0.069	Simple	0.46	6.2	5.1e6	6.8e3	0.9	0.6	1183	15	72	16.6	0.06	2.4	1.1	Moderate
	P1-shot 2	250	5.3	4.5	8000	8.5e4	0.66	0.069	Simple	0.46	6.2	5.1e6	6.8e3	0.9	0.6	1183	167	350	192	0.27	13.4	6.1	Haz Fail
	P2	250	5.3	4.5	8000	8.5e4	0.66	0.069	Simple	0.46	6.2	5.1e6	6.8e3	0.9	0.6	1183	8	76	9.6	0.07	2.4	1.1	Moderate
	P3	250	5.3	4.5	8000	8.5e4	0.66	0.069	Simple	0.46	6.2	5.1e6	6.8e3	0.9	0.6	1183	56	224	64.3	0.18	11.8	5.4	Heavy
	P5	250	5.3	4.5	8000	8.5e4	0.66	0.069	Simple	0.46	6.2	5.1e6	6.8e3	0.9	0.6	1183	15	124	16.9	0.11	4.9	2.2	Moderate
	P6	250	5.3	4.5	8000	8.5e4	0.66	0.069	Simple	0.46	6.2	5.1e6	6.8e3	0.9	0.6	1183	3	36	3.4	0.03	0.6	0.3	Superfcl
Airblast Loading on Wall Panels	150-1	94	5.9	5.0	6000	7.7e4	0.21	0.027	Simple	0.51	8.6	4.4e6	3.9e3	3.6	37.4	1316	62	116	17.5	0.09	1.8	2.2	Moderate
	150-2	94	5.9	5.0	6000	7.7e4	0.21	0.027	Simple	0.51	8.6	4.4e6	3.9e3	3.6	37.5	1317	234	227	65.6	0.19	4.5	5.4	Heavy
	200-1	94	7.9	7.0	4400	7.7e4	0.26	0.041	Simple	0.68	20.3	3.8e6	8.7e3	7.9	75.7	1753	1008	528	128	0.31	3.9	4.7	Heavy
	200-2	94	7.9	7.0	4400	7.7e4	0.26	0.041	Simple	0.68	20.3	3.8e6	8.7e33	7.9	75.7	1753	1008	528	128	0.31	3.6	4.4	Heavy
	200-3	94	7.9	7.0	4400	7.7e4	0.26	0.041	Simple	0.68	20.3	3.8e6	8.7e3	7.9	75.7	1753	1008	528	128	0.31	3.8	4.6	Heavy
	200-4	94	7.9	7.0	4400	7.7e4	0.26	0.041	Simple	0.68	20.3	3.8e6	8.7e3	7.9	75.7	1753	219	227	27.8	0.12	2.1	2.5	Moderate
	200-5	94	7.9	7.0	4400	7.7e4	0.26	0.041	Simple	0.68	20.3	3.8e6	8.7e3	7.9	75.7	1753	529	311	67.2	0.17	2.2	2.6	Moderate
	200-6	94	7.9	7.0	4400	7.7e4	0.26	0.041	Simple	0.68	20.3	3.8e6	8.7e3	7.9	75.7	1753	1008	528	128	0.31	3.1	3.8	Heavy
	200-7	94	7.9	7.0	4400	7.7e4	0.26	0.041	Simple	0.68	20.3	3.8e6	8.7e3	7.9	75.7	1753	1008	528	128	0.31	3.0	3.7	Heavy
	200-8	94	7.9	7.0	4400	7.7e4	0.26	0.041	Simple	0.68	20.3	3.8e6	8.7e3	7.9	75.7	1753	1008	528	128	0.31	3.1	3.7	Heavy
	200-9	94	7.9	7.0	4400	7.7e4	0.26	0.041	Simple	0.68	20.3	3.8e6	8.7e3	7.9	75.7	1753	1008	528	128	0.31	3.7	4.5	Heavy
WES Semi - Hardened Facility Design Criteria Tests	Test I-1	65	12.8	11.0	6000	8.5e4	1.00	0.141	Fixed	1.10	87.3	4.4e6	9.5e4	360	6644	2851	2960	916	8.2	0.07	0.6	1.0	Moderate
	Test I-2	65	12.8	11.0	6000	8.5e4	0.50	0.071	Fixed	1.10	87.3	4.4e6	5.0e4	188	6644	2851	2960	916	15.7	0.10	1.0	1.8	Moderate
	Test I-3	65	12.8	11.0	6000	8.5e4	0.50	0.071	Fixed	1.10	87.3	4.4e6	5.0e4	188	6644	2851	2960	916	15.7	0.10	3.0	5.3	Heavy
	Test I-4	65	12.8	11.0	6000	8.5e4	0.25	0.035	Fixed	1.10	87.3	4.4e6	2.5e4	96	6644	2851	2960	916	30.8	0.16	2.2	4.0	Heavy
	Test I-6	65	12.8	11.0	6000	8.5e4	0.25	0.035	Fixed	1.10	87.3	4.4e6	2.5e4	96	6644	2851	2960	916	30.8	0.16	1.5	2.6	Moderate